Chin. J. Astron. Astrophys. Vol. 7 (2007), No. 1, 51–62
(*http://www.chjaa.org*)

Chinese Journal of
Astronomy and
Astrophysics

Note on Redshift Distortion in Fourier Space *

Yan-Chuan Cai[1,2] and Jun Pan[1]

[1] Purple Mountain Observatory, Chinese Academy of Sciences, Nanjing 210008; *jpan@pmo.ac.cn*
[2] National Astronomical Observatories, Chinese Academy of Sciences, Beijing 100012

Received 2006 April 17; accepted 2006 June 20

Abstract We explore features of redshift distortion in Fourier analysis of N-body simulations. The phases of the Fourier modes of dark matter density fluctuation are generally shifted by the peculiar motion along the line of sight, the induced phase shift is stochastic and has a probability distribution function (PDF) that is symmetric about the peak at zero shift and whose exact shape depends on the wave vector, except on very large scales where phases are invariant by linear perturbation theory. Analysis of the phase shifts motivates our phenomenological models for the bispectrum in redshift space. Comparison with simulations shows that our toy models are very successful in modeling bispectrum of equilateral and isosceles triangles at large scales. In the second part we compare the monopole of the power spectrum and bispectrum in the radial and plane-parallel distortion to test the plane-parallel approximation. We confirm the results of Scoccimarro that difference of power spectrum is at the level of 10%, and, in the reduced bispectrum, the difference is as small as a few percent. However, on the plane perpendicular to the line of sight of $k_z = 0$, the difference in power spectrum between the radial and plane-parallel approximation can be more than $\sim 10\%$, and even worse on very small scales. Such difference is prominent for bispectrum, especially for configurations of tilted triangles. Non-Gaussian signals under the radial distortion on small scales are systematically biased downside than are in the plane-parallel approximation, with amplitudes depending on the opening angle of the sample point to the observer. This observation gives warning to the practice of using the power spectrum and bispectrum measured on the $k_z = 0$ plane as estimates of the real space statistics.

Key words: cosmology: theory — large-scale structure of universe — methods: statistical

1 INTRODUCTION

Large redshift surveys of galaxies provide us with distances estimated from measured redshifts to complete our three-dimensional topography of the visible universe. However, due to the peculiar velocities of galaxies, the inferred redshift from the observation is not an exact indication of the true distance, our statistical estimation in the redshift space thus suffers from redshift distortion. On large scales the peculiar velocities are dominated by bulk inflow and the redshift distortion boosts the clustering strength of galaxies; on small scales the virialized peculiar velocities suppress the clustering power and account for the phenomenon of "Finger of God" (e.g. Kaiser 1987; Hamilton 1998).

Redshift distortion is entangled with bias and the gravitational nonlinearity. Nevertheless, fruitful results of redshift distortion have been achieved and applied in statistical analysis of large scale structure (LSS), particularly the power spectrum $P(k)$ and the two point correlation function ξ. On large scales where linear theory applies, the power spectrum in redshift space is

$$P_s(\boldsymbol{k}) = (1 + \beta\mu^2)^2 P(k) \,, \tag{1}$$

∗ Supported by the National Natural Science Foundation of China.

where $\beta = \Omega_m^{0.6}/b$ with b the linear bias parameter, and μ is the cosine of the angle between $\boldsymbol{k}$ and the unit vector $\hat{z}$ of line-of-sight (LOS) (Kaiser 1987). Further observation and analysis of N-body simulation indicate that over wide scales including strong nonlinear regime there is an accurate empirical formula to model the effect of redshift distortion on the power spectrum with introduction of a pairwise velocity dispersion parameter σ_v (e.g. Park et al. 1994; Peacock & Dodds 1994; Cole, Fisher & Weinberg 1995; Hatton & Cole 1998; White 2001),

$$P_s(\boldsymbol{k}) = P(k)\frac{(1+\beta\mu^2)^2}{[1+(k\mu\sigma_v)^2/2]^2} \ . \tag{2}$$

In comparison, our understanding of redshift distortions for bispectrum or the three point correlation function is not satisfactory (Hivon et al. 1995; Verde et al. 1998; Scoccimarro et al. 1999), which, in part, is attributed to the non-perturbative nature of redshift distortion effect (Scoccimarro et al. 1999). The intrinsic difference between power spectrum and bispectrum is that power spectrum is a phase invariant quantity which contains only the information of the amplitude of the Fourier transform of the density contrast, while bispectrum consists of contributions from both amplitudes and phases (Matsubara 2003). Research based on phases has revealed that phase information is very crucial in LSS distribution pattern recognition (Chiang & Coles 2000; Chiang 2001; Chiang, Coles & Naselsky 2002), especially for the bispectrum and the three point correlation function (Watts & Coles 2003; Watts, Coles & Melott 2003; Matsubara 2003; Hikage, Matsubara & Suto 2004; Chiang 2004; Hikage et al. 2005). Therefore there is strong reason to believe that the behavior of phases under redshift distortion will provide us with precious information, which is the starting point of this paper.

An alternative route to tackle the redshift distortion is to recover real space quantities from measurements in the redshift space. The anisotropic two point correlation function in redshift space $\xi(\boldsymbol{s})$ is measured along two separations as $\xi(\sigma,\pi)$, where $\pi = \boldsymbol{s}\cdot\hat{z}/s$ and $\sigma = |\boldsymbol{s}\times\hat{z}|/s$. The projected two point correlation function $\Xi(\sigma)$ is free of redshift distortion and is simply related to the real space $\xi(r)$ by (Davis & Peebles 1983; Fisher et al. 1994)

$$\Xi(\sigma) \equiv \int_{-\infty}^{+\infty}\xi(\sigma,\pi)d\pi = 2\int_{\sigma}^{+\infty}\frac{r\xi(r)dr}{(r^2-\sigma^2)^{\frac{1}{2}}} \ , \tag{3}$$

or, we can deproject Ξ to get the real space two point correlation function (e.g. Saunders, Rowan-Robinson & Lawrence 1992; Hawkins et al. 2003)

$$\xi(r) = -\frac{1}{\pi}\int_{r}^{+\infty}\frac{d\Xi(\sigma)/d\sigma}{(\sigma^2-r^2)^{\frac{1}{2}}}d\sigma \ . \tag{4}$$

In Fourier space it is much simpler, as we can see from Equations (1) and (2) that if we restrict our measurement on the plane of $k_z = 0$ only, what we obtain is the real space power spectrum (e.g. Park et al. 1994; Hamilton & Tegmark 2002).

However, this approach relies on the assumption of the parallel approximation, i.e., the observer is at infinite distance so the unit vector $\hat{z}$ of the LOS is pointing to a fixed direction. In reality there is no such fixed direction of LOS, systematic biases are inevitably introduced in the treatment mentioned above. In particular, since Fourier transform mixes all scales together, even at high k there is some contamination from scales at wide angles. Consequently, not only are polyspectra measured on $k_z = 0$ plane not equivalent to those in real space, but also the monopoles of the polyspectra with respect to the LOS are not strictly following what theories of redshift distortion predict under the plane approximation. Further complication also arises that Fourier modes are no longer independent and the covariance matrix is not diagonal (Zaroubi & Hoffman 1996; Scoccimarro 2000).

Attention has been called in works analyzing galaxy redshift surveys which always subtend wide angles over sky and are at low redshift, to reduce the systematics in the adoption of the parallel approximation. Numerical studies have shown that if one confines to working with small angles, differences caused by the parallel approximation are negligible in monopoles, in quadruples of the power spectrum are usually under $\sim 5\%$ if the opening angle of the window in which the Fourier transform is performed is less than 50° (e.g.

Park et al. 1994; Cole, Fisher & Weinberg 1994). Scoccimarro (2000) also reported that this approximation was good enough for measuring the monopoles of the power spectrum and the bispectrum. Even for all sky surveys the difference is as small as 10%. Whatsoever, as the parallel approximation plays a fundamental role in Fourier analysis of the spatial distribution of galaxies, it definitely deserves an in-depth study, crucial for confidence in our interpretation of what we estimate in redshift space. We will show in this paper that real life is never simple.

This paper is organized as follows. In Section 2, we give a general description of mapping from real space to redshift space, and demonstrate the shift of phases of Fourier modes by redshift distortion and discuss possible construction of empirical model for bispectrum in redshift space. Section 3 focuses on the difference between the plane-parallel approximation and the radial distortion. Section 4 presents our conclusions and a discussion. Throughout the paper we use two sets of ΛCDM simulations by the Virgo consortium, the Virgo simulation in boxes of size $239.5\,h^{-1}$ Mpc with 256^3 particles and the very large simulation (VLS) in boxes of size $479\,h^{-1}$ Mpc with 512^3 particles, with the cosmological parameters $\Omega_m = 0.3$, $\Omega_\Lambda = 0.7$, $\sigma_8 = 0.9$ and $\Gamma = 0.21$ (Jenkins et al. 1998).

2 PHASE INFORMATION AND BISPECTRUM IN REDSHIFT SPACE

2.1 Phase Shift is a Nonlinear Effect

For simplicity we adopt in this section the plane approximation so the unit vector of LOS $\hat{z}$ has a fixed direction. The mapping from real space coordinates $\boldsymbol{r}$ to redshift space $\boldsymbol{s}$ is

$$\boldsymbol{s} = \boldsymbol{r} - \beta \boldsymbol{u}_z(\boldsymbol{r})\hat{z}\ , \tag{5}$$

where $\boldsymbol{u}(\boldsymbol{r}) \equiv -\boldsymbol{v}(\boldsymbol{r})/(\mathcal{H}\beta)$, $\boldsymbol{v}(\boldsymbol{r})$ is the peculiar velocity, and $\mathcal{H}(\tau) \equiv (1/a)(da/d\tau) = Ha$ is the conformal Hubble parameter with FRW scale factor a and conformal time τ (Scoccimarro et al. 1999; Scoccimarro 2004).

The density contrast in redshift space, $\delta_s(s)$, is obtained from the real space density fluctuation $\delta(r)$ by requiring conservation of the number of galaxies,

$$(1+\delta_s)d^3s = (1+\delta)d^3r. \tag{6}$$

The Fourier transform of the number density contrast in redshift space reads

$$\delta_s(\boldsymbol{k}) \equiv \int \frac{d^3s}{(2\pi)^3} \mathrm{e}^{-i\boldsymbol{k}\cdot\boldsymbol{s}} \delta_s(\boldsymbol{s}) = \int \frac{d^3x}{(2\pi)^3} \mathrm{e}^{-i\boldsymbol{k}\cdot\boldsymbol{x}} \mathrm{e}^{i\beta k_z u(x)} \left[\delta(\boldsymbol{x}) + \beta\nabla_z u_z(x)\right]\ , \tag{7}$$

in which and hereafter the subscript "s" refers to quantities in redshift space. The term in square brackets describes the squashing effect, i.e., the boost to the clustering amplitude, whereas the exponential factor encodes the "Finger of God" effect, which erases power due to velocity dispersion along the LOS. In plane-parallel approximation, the distortion comes from the peculiar velocity along the LOS v_z. Thus, to generate a redshift space sample, we only need $s_z = r_z - \beta u_z$.

It is clear from Equation (7) that in the redshift space, not only the amplitude $|\delta(k)|$, but also the phase angle $\theta(k)$ is distorted, which is casually ignored. The expression can be expanded perturbatively as demonstrated by Soccimarro et al. (1999) who calculated the expansion to second order to model the bispectrum in redshift space on large scales. We reproduce here the expansion

$$\delta_s(\boldsymbol{k}) = \sum_{n=1}^{\infty} \int d^3k_1 ... d^3k_n [\delta_D]_n \left[\delta(\boldsymbol{k}_1) + \beta\mu_1^2\phi(\boldsymbol{k}_1)\right] \frac{(\beta\mu k)^{n-1}}{(n-1)!} \frac{\mu_2}{k_2}\phi(\boldsymbol{k}_2) ... \frac{\mu_n}{k_n}\phi(\boldsymbol{k}_n)\ , \tag{8}$$

where $[\delta_D]_n = \delta_D(\boldsymbol{k} - \boldsymbol{k}_1 - ... - \boldsymbol{k}_n)$ is the Dirac function, velocity divergence is $\phi(\boldsymbol{r}) \equiv \nabla\cdot\boldsymbol{u}$ and $\mu_n = \boldsymbol{k}_n\cdot\hat{z}/k_n$. In the linear theory, only the first order $n = 1$ counts, and we recover the well-known Kaiser formula (Kaiser 1987)

$$\delta_s(\boldsymbol{k}) = (1+\beta\mu^2)\delta(\boldsymbol{k})\ , \tag{9}$$

which tells that at the first order phases are not changed by the redshift distortion, phase shift is a phenomenon at high orders $n \geq 2$, i.e. nonlinear. We are not going to calculate quantitatively the phase shift in perturbation theory, rather, as a starting point in this direction, we aim at presenting the existence of the phase shift in numerical simulations and hence implications drawn from the information to understand redshift distortion on phase-related statistics, the bispectrum.

2.2 Bispectrum and Phase Information

By definition, the bispectrum is the ensemble average of the product of three Fourier modes with their wave vectors forming a triangle,

$$B(\boldsymbol{k}_1, \boldsymbol{k}_2, \boldsymbol{k}_3 = -\boldsymbol{k}_1 - \boldsymbol{k}_2) = \langle \delta(\boldsymbol{k}_1)\delta(\boldsymbol{k}_2)\delta^*(\boldsymbol{k}_3)\rangle \ = \langle |\delta_1||\delta_2||\delta_3| e^{i(\theta_1+\theta_2-\theta_3)}\rangle \ , \tag{10}$$

where we wrote the Fourier mode $\delta(\boldsymbol{k}) = |\delta| e^{i\theta}$. It is well known that the nonlinearity of gravitational evolution generates correlation between the phase θ and the amplitude $|\delta|$ as well as correlations between different modes, especially on small scales, although in the initial fluctuation there are no such correlations. Whilst we are living with such universal correlations, on large scales where the nonlinearity is fairly weak, keeping the correlation between different modes to ensure non-zero bispectrum we can make an assumption to neglect the correlation between the amplitude and the phase of a single mode, an interesting conclusion emerges. With the assumption, the ensemble average of bispectrum can be decomposed into

$$B(\boldsymbol{k}_1, \boldsymbol{k}_2, \boldsymbol{k}_3) \propto \langle |\delta_1||\delta_2||\delta_3|\rangle \int e^{i\Theta} p(\Theta) d\Theta \ , \tag{11}$$

in which $p(\Theta)$ is the PDF of the phase sum $\Theta = \theta_1 + \theta_2 - \theta_3$. Since the bispectrum is real and $\delta(\boldsymbol{k})$ is Fourier transform of a real function, $p(\Theta)$ will be symmetric to $\Theta = 0$ and can be expanded as $p(\Theta) = c_0 + \sum_n c_n \cos(n\Theta)$. Keeping only the first two terms, we recover the essence of the results of Matsubara (2003)

$$p(\Theta) \propto (1 + \mathrm{const} \cdot \cos\Theta) \ . \tag{12}$$

In redshift space, modifications occur in both amplitudes and phases,

$$\delta_s(\boldsymbol{k}) = |\delta_s| e^{i\theta_s} = \alpha(\boldsymbol{k}) |\delta(\boldsymbol{k})| e^{i(\theta+\Delta\theta)} \ , \tag{13}$$

in which the amplification factor $\alpha(\boldsymbol{k}, \mu)$ is real and phase shift is $\Delta\theta(\boldsymbol{k}) \equiv \theta_s(\boldsymbol{k}) - \theta(\boldsymbol{k})$. Thus the bispectrum in redshift space can be written as

$$B_s(\boldsymbol{k}_1, \boldsymbol{k}_2, \boldsymbol{k}_3 = -\boldsymbol{k}_1 - \boldsymbol{k}_2) = \langle \alpha_1\alpha_2\alpha_3 |\delta_1||\delta_2||\delta_3| e^{i(\theta_1+\theta_2-\theta_3)} e^{i(\Delta\theta_1+\Delta\theta_2-\Delta\theta_3)}\rangle \ . \tag{14}$$

According to our observation of the Virgo and the VLS simulations, $\alpha(\boldsymbol{k}) = \alpha(k, \mu)$ is deterministic and can be well approximated by $\alpha = (1 + \beta\mu^2)/[1 + (k\mu\sigma_v)^2/2]$ as in Equation (2), hence the product of amplitude amplification factors in Equation (14) can be placed outside the ensemble average.

If we assume at a given $\boldsymbol{k}$, $\Delta\theta$ is fixed regardless of the original stochastics, $\Delta\Theta = \Delta\theta_1 + \Delta\theta_2 - \Delta\theta_3$ will be a constant, so that $B_s = \alpha_1\alpha_2\alpha_3 B e^{i\Delta\Theta}$. $\Delta\Theta$ has to be $n\pi$ ($n = 0, \pm1, \pm2...$) as B_s is real, so

$$B_s = \alpha_1\alpha_2\alpha_3 B \ . \tag{15}$$

It is hard to conjecture there is a cosmic conspiracy to satisfy $\Delta\Theta = n\pi$ for arbitrary $(\boldsymbol{k}_1, \boldsymbol{k}_2, \boldsymbol{k}_3)$ triplet, the only possibility is for any mode $\Delta\theta = n\pi$, which is obviously impossible as implied by Equations (7) and (8). The immediate conclusion is that the phase shift resulting from the redshift distortion has dependence on the phase in real space and therefore is stochastic.

In the N-body simulations we found that although the phases are uniformly distributed in both real space and redshift space, the distribution of phase shift $p(\Delta\theta)$ is not uniform as shown in Figure 1. In general $p(\Delta\theta)$ depends on (k, μ) and is peaked at the center, $\Delta\theta = 0$. As μ or k decreases, the dispersion of the distribution gets smaller and more modes concentrate in the vicinity of $\Delta\theta = 0$. This is easy to understand since those modes around the plane perpendicular to LOS suffer little from redshift distortion (Eq. (7)) while on large scales the deviation to linear redshift distortion theory of Equation (9) becomes small. We examined that in the simulations the phases of modes on the plane $\mu = 0$ are unshifted.

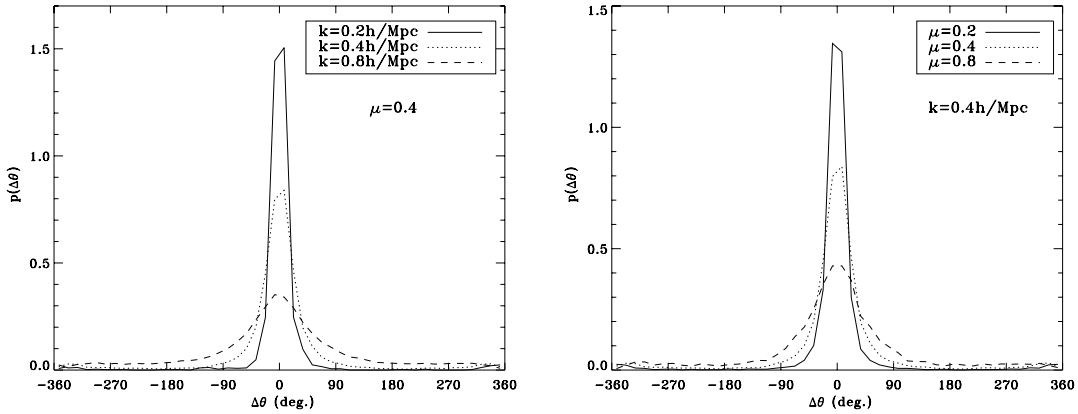

Fig. 1 Probability distribution functions of phase shift $\Delta\theta$ resulting from redshift distortion in N-body simulations. The left panel plots the $p(\Delta\theta)$ for different k scales at fixed $\mu = \boldsymbol{k} \cdot \hat{z}/k$, and the right panel, for different μ values at fixed $k = 0.4\,h\,\mathrm{Mpc}^{-1}$.

2.3 Toy Models for Bispectrum in Redshift Space

In an attempt to understand the redshift distortion of bispectrum, by way of a crude approximation in the spirit of deriving Equation (12) we assume that $\Delta\Theta$ is uncorrelated with $|\delta_{1,2,3}|$ and $\theta_{1,2,3}$, which is possible since $\Delta\Theta$ is a sum of three random variables. Equation (14) then becomes $B_s = B \times \alpha_1\alpha_2\alpha_3 \int e^{i\Delta\Theta} p(\Delta\Theta) d\Delta\Theta$, and $p(\Delta\Theta) \propto (1 + \mathrm{const} \cdot \cos\Delta\Theta)$, if high order terms are ignored. With a further assumption that $\Delta\theta_{1,2,3}$ are independent of each other, we have

$$\begin{aligned} B_s(\boldsymbol{k}_1, \boldsymbol{k}_2, \boldsymbol{k}_3) =& B(\boldsymbol{k}_1, \boldsymbol{k}_2, \boldsymbol{k}_3) \times \alpha_1\alpha_2\alpha_3 \\ & \times \int e^{i\Delta\theta_1} p(\Delta\theta_1) d\Delta\theta_1 \int e^{i\Delta\theta_2} p(\Delta\theta_2) d\Delta\theta_2 \int e^{i\Delta\theta_3} p(\Delta\theta_3) d\Delta\theta_3 \,, \end{aligned} \tag{16}$$

from which trivially we again have $p(\Delta\theta)$ being symmetric to $\Delta\theta = 0$, as seen in Figure 1 and $\propto (1 + \mathrm{const} \cdot \cos\Delta\theta)$. Note that here α and $\Delta\theta$ are functions of two variables (k, μ). Equation (16) is quite similar to the phenomenological model of Scoccimarro et al. (1999), and it serves as a theoretical support to their *ansatz*.

In practice it is often simpler to measure the bispectrum averaged over all possible combinations of wave vectors $(\boldsymbol{k}_1, \boldsymbol{k}_2, \boldsymbol{k}_3 = -\boldsymbol{k}_1 - \boldsymbol{k}_2)$ with fixed $k_1 = |\boldsymbol{k}_1|$, $k_2 = |\boldsymbol{k}_2|$ and angle $\psi = \boldsymbol{k}_1 \cdot \boldsymbol{k}_2/(k_1 k_2)$. In real space it is the isotropic bispectrum $B(k_1, k_2, k_3) = B(\boldsymbol{k}_1, \boldsymbol{k}_2, \boldsymbol{k}_3)$, in redshift space, due to the anisotropy of redshift distortion, the angle-average with respect to LOS is the monopole of the true bispectrum $B_s(k_1, k_2, \psi, \mu_1, \mu_2, \mu_3)$. Here, we denote the azimuthal angle of $\boldsymbol{k}_2$ about $\boldsymbol{k}_1$ by φ, and

$$\begin{aligned} \mu_1 &= \mu = \boldsymbol{k}_1 \cdot \hat{z}/k_1 \,, \\ \mu_2 &= \mu\cos\psi - \sqrt{1-\mu^2}\sin\psi\cos\varphi \,, \\ \mu_3 &= -\frac{k_1}{k_3}\mu - \frac{k_2}{k_3}\mu_2 \,, \end{aligned} \tag{17}$$

the monopole of bispectrum in redshift space is

$$B_s^{(0)}(k_1, k_2, \psi) = \frac{1}{4\pi}\int_{-1}^{1} d\mu \int_0^{2\pi} d\varphi B_s(k_1, k_2, \psi, \mu, \varphi) \,. \tag{18}$$

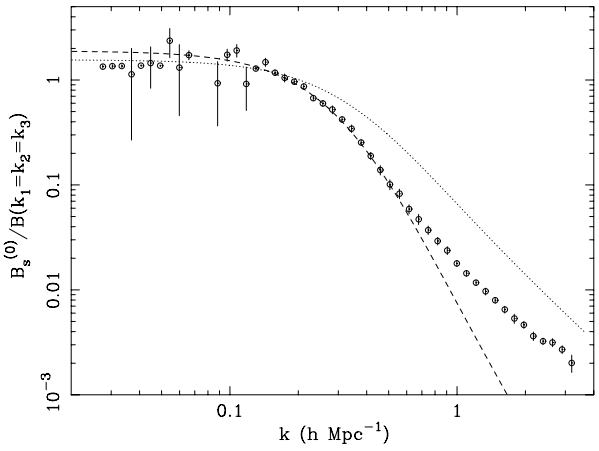

Fig. 2 $B_s^{(0)}/B$ of equilateral triangles. Dotted line is the prediction of Eq. (19), and dash line is the empirical model of Eq. (20). Points are averaged over measurement of the Virgo simulation and the eight subsets of the VLS simulation. Error bars are 1σ scatter.

On large scales where the nonlinearity is weak and phases shifts are close to zero (Eq. (9) and Fig. 1), we can approximate the modulation by peculiar velocity with Equation (15),

$$\frac{B_s^{(0)}}{B} = \frac{1}{4\pi}\int_{-1}^{1}\int_{0}^{2\pi} \alpha(k_1,\mu)\alpha(k_2,\mu,\psi,\varphi)\alpha(k_3,\mu,\psi,\varphi)d\varphi\, d\mu. \tag{19}$$

We measured angle-averaged power spectrum and bispectrum both in real space and redshift space for the Virgo simulation and eight subsets of the VLS simulation which are generated by dividing the VLS simulation into independent cubes of half of the original box size. From power spectra with Equation (2), $\sigma_v = 4.87$ is fitted, and then is inserted into Equation (19) as our toy model for $B_s^{(0)}$.

In Figure 2 it is interesting to observe the remarkable agreement of our toy model based on phase information with simulations for equilateral triangles for $k < 0.2\,h\,\mathrm{Mpc}^{-1}$ beyond which tree-level perturbation theory and the second order Lagrangian theory also break down (Scoccimarro 2000). As k grows, the phase shift is no longer negligible and our toy model fails.

As a next level beyond the simple prescription of Equation (19), a better approximation may be achieved through integration of Equation (16) instead of the simple formula of Equation (19) if we know $p(\Delta\theta)$, which carries important information about the redshift distortion and numerically, depends more on (k,μ) (Fig. 1). Because we are not equipped with a whole battery of many simulations in very large boxes, so far we are not able to develop functional expression to fit $p(\Delta\Theta)$ allowing for their dependence on (k,μ) and σ_v. Nevertheless, we can parameterize the toy model in a simple way to improve its performance just as in Scoccimarro et al. (1999), e.g.,

$$\frac{B_s^{(0)}}{B} = A_1\left[\frac{1}{4\pi}\int_{-1}^{1}\int_{0}^{2\pi} \alpha(k_1,\mu)\alpha(k_2,\mu,\psi,\varphi)\alpha(k_3,\mu,\psi,\varphi)d\varphi\, d\mu\right]^{A_2}, \tag{20}$$

with two fitting parameters $A_{1,2}$. An eye-ball examination with $A_1 = 1/1.15$ and $A_2 = 1.75$ does improve agreement up to scale $k \sim 0.5\,h\,\mathrm{Mpc}^{-1}$ for equilateral triangles (Fig. 2). We then compare the modified toy model for other configurations with simulations in Figure 3. We see that for isosceles with $\psi >\sim 90^\circ$ the agreement of our modified toy model with simulations is very impressive too, although for very tilted configuration with $k_2/k_1 \geq 2$ the differences are huge. We are not intending to give accurate fit, but are just demonstrating the possibility of constructing a good approximation model with the simple prescription of Equation (19), and, in the mean time showing the discrepancy due to our rough handling of the phase shift.

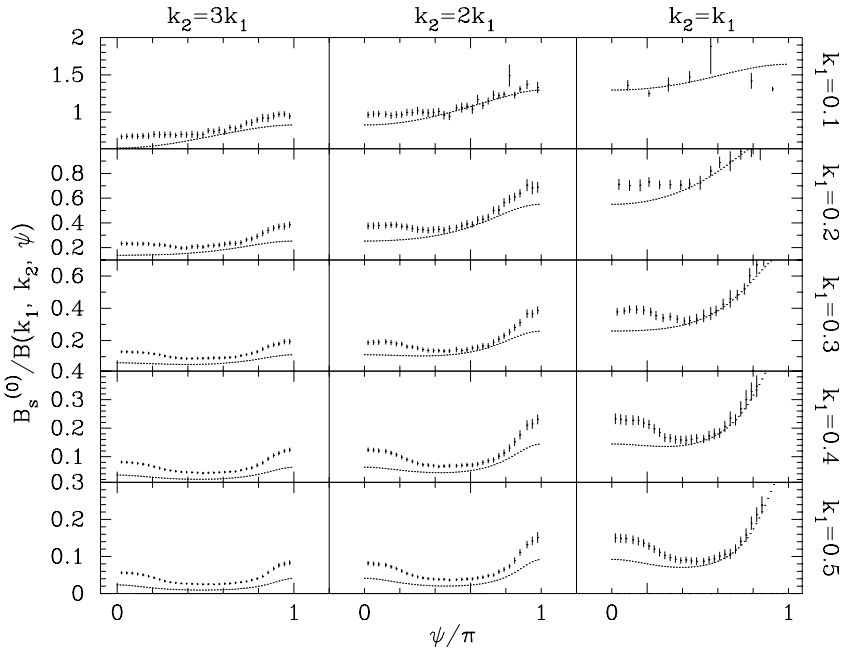

Fig. 3 $B_s^{(0)}/B(k_1, k_2, \psi)$ of different configurations. The dotted line is our modified toy model Eq. (20), see Fig. 2 for other keys.

3 GOODNESS OF PLANE-PARALLEL APPROXIMATION TO RADIAL DISTORTION

So far we are working with the plane-parallel approximation. As we have addressed in Section 1, this approximation is appropriate when the angle subtended by the sample is small. When dealing with large samples, especially all sky surveys, radial distortion should be taken into account. To investigate the goodness of the plane-parallel approximation to the exact radial distortion, we shall compare a set of power spectra and bispectra in redshift space in the parallel approximation and the radial distortion.

3.1 Monopoles of Power Spectrum and Bispectrum

It has been shown by Scoccimarro (2000) that the monopoles of power spectrum and bispectrum of an all sky survey, in the radial and the plane-parallel distortions, are consistent with each other within the error bars. For the power spectrum the difference is within $\sim 10\%$ and for the bispectrum is within a few percents.

To generate samples in redshift space in radial distortion, we strictly follow Equation (5) with $\hat{z}$ defined by the unit vector pointing from the observer to the point sampled, i.e., $\hat{z}$ is simply the unit position vector $\hat{\boldsymbol{r}}$. Cartesian coordinates $r_{i=1,2,3}$ of any point in our sample are within $[0, L]\, h^{-1}\,\mathrm{Mpc}$, $L = 239.5$. In this subsection, we placed the observer at $(0.5\sqrt{2}L, 0.5\sqrt{2}L, -100)\, h^{-1}\,\mathrm{Mpc}$, the largest angle of the sample opening to the observer is $118.88°$. Then points in samples are transformed into the coordinate system in which the observer is sitting at the origin. For every data point we have redshift from the Hubble flow $z_{\,\mathrm{Hub}}$ and an induced peculiar velocity z_{pec}, the comoving distance in redshift space s is then calculated from the final redshift $z = (1 + z_{\mathrm{Hub}})(1 + z_{\mathrm{pec}}) - 1$, while its orientation does not change.

In Figure 4, we plot the ratio of the monopoles of power spectra in radial distortion and the parallel approximation, $P_{\mathrm{r}}^{(0)}/P_{\mathrm{p}}^{(0)}$, where the subscript "r" means radial distortion, "p" refers to parallel approximation and all polyspectra are in redshift space if not specified explicitly. Monopole of power spectrum is defined as the angular average of the anisotropic $P(\boldsymbol{k})$. Comparison of the monopoles of reduced bispectrum is illustrated in Figure 5. Note that the monopole of reduce bispectrum is given by

$$Q^{(0)}(k_1, k_2, \psi) = \frac{B^{(0)}(k_1, k_2, \psi)}{P^{(0)}(k_1)P^{(0)}(k_2) + P^{(0)}(k_2)P^{(0)}(k_3) + P^{(0)}(k_3)P^{(0)}(k_1)}\,. \tag{21}$$

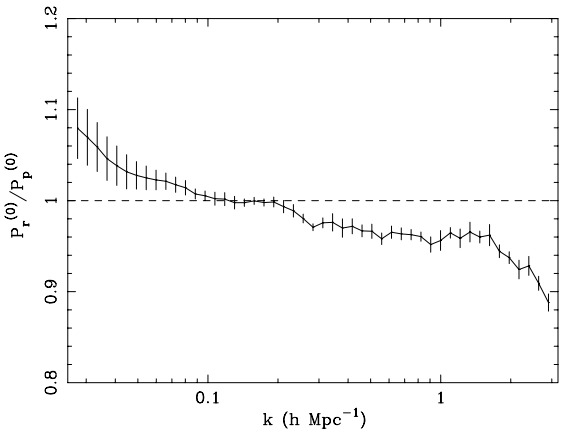

Fig. 4 Ratio of the monopoles of power spectra in radial distortion and parallel approximation. The sample is at distance $100\,h^{-1}$ Mpc.

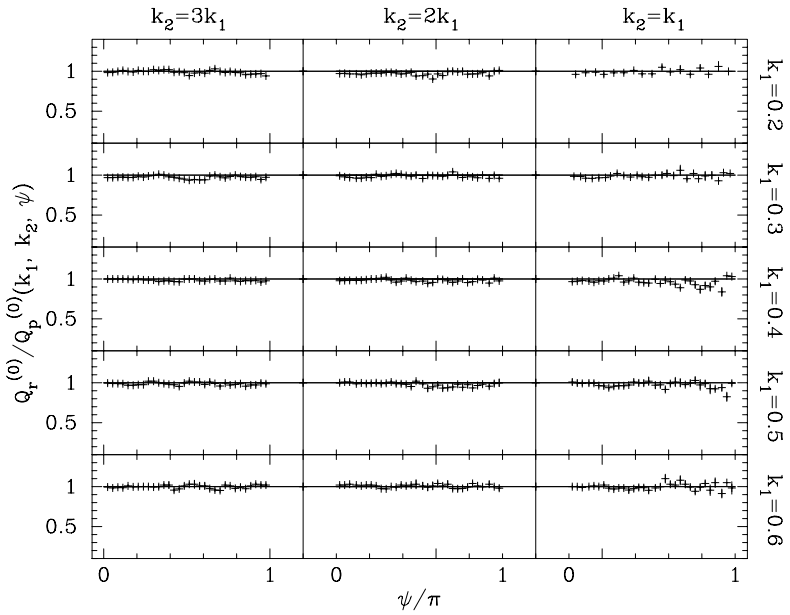

Fig. 5 $Q_{\rm r}^{(0)}/Q_{\rm p}^{(0)}(k_1, k_2, \psi)$ for triangles of $k_1 = 0.2, 0.3, 0.4, 0.5$ and $0.6\,h\,{\rm Mpc}^{-1}$, and $k_2/k_1 = 1, 2, 3$. The observer is at distance $100\,h^{-1}$ Mpc.

We can see from Figure 4 that the differences between monopoles of power spectrum in the radial and the plane-parallel distortion are within 10%, while the differences for bispectra are a few percents (Fig. 5). These results confirm the assertion of Zaroubi & Hoffman (1996) and Scoccimarro (2000). As shown in Figure 4, the power in parallel approximation on large scales ($k < 0.1\,h\ {\rm Mpc}^{-1}$) is smaller than that under radial distortion. On the other hand, on small scales ($k > 0.2\,h\,{\rm Mpc}^{-1}$), the plane-parallel distorted power spectrum is larger. This is because in the plane-parallel approximation there is no distortion effect along directions perpendicular to the fixed LOS, the actual redshift distortion is radial and the LOS is not fixed. Distortion is more severe to structure clumps so that there are greater effects of boost at large scales and suppression at small scales on the clustering strength.

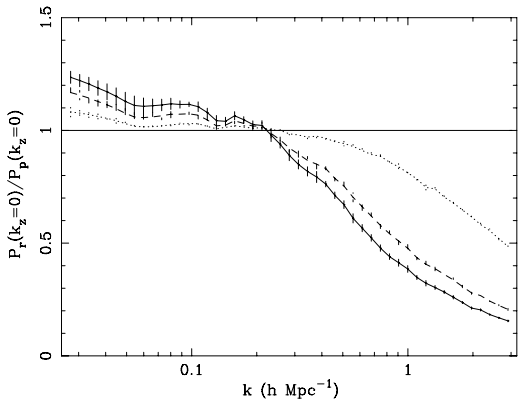

Fig. 6 Ratios of power spectra for radial and parallel distortion on the plane of $k_z = 0$. The solid line, dash line and dot line are for samples at distances of $100\,h\,\mathrm{Mpc}^{-1}$, $200\,h\,\mathrm{Mpc}^{-1}$ and $1000\,h\,\mathrm{Mpc}^{-1}$ to the observer, respectively.

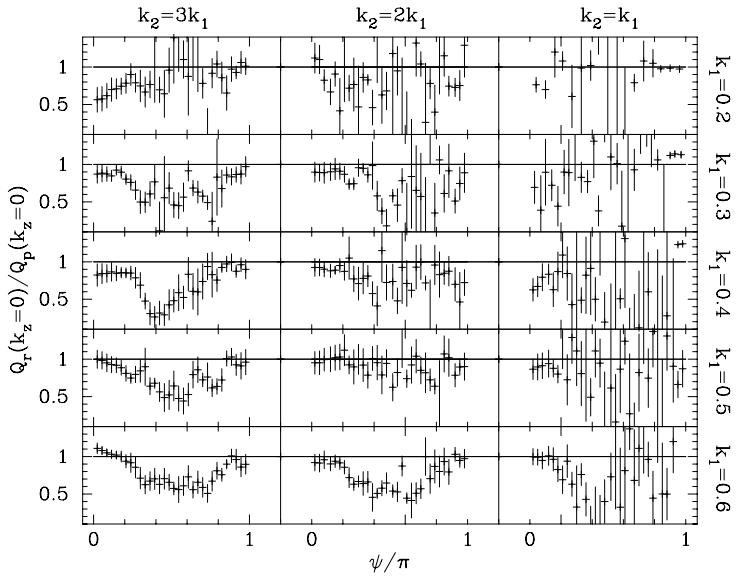

Fig. 7 Ratios of reduced bispectra for radial and parallel distortion on the plane of $k_z = 0$. Observer is located at the distance of $100\,h^{-1}$ Mpc.

3.2 Power Spectrum and Bispectrum on the Plane of $k_z = 0$

We have seen there is systematic bias caused by the parallel approximation to the radial distortion in monopoles of power spectrum and bispectrum, although it is very weak. In this subsection we set about to explore the behavior of the polyspectra on the plane of $k_z = 0$ that are regarded as estimation of the real space quantities in the plane-parallel approximation. It is easy to understand that on large scales where the opening angle to the observer is wide so the lines of sight can not be approximated by parallel lines, such deviation is not separable in Fourier transform which is a global operation. Only when the opening angle of the sample window is small are we safe. In order to check the influence of the opening angle of sample to the method of using polyspectra of $k_z = 0$ as estimates in real space, we created different samples in redshift space from the simulations by placing the observer at distances of 100, 200 and $1000\,h^{-1}$ Mpc, respectively.

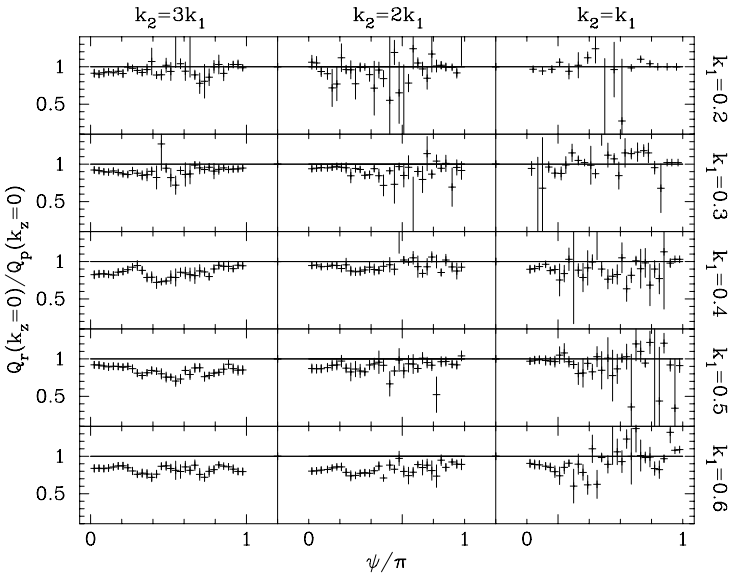

Fig. 8 Ratios of reduced bispectra for radial and parallel distortion on the plane of $k_z = 0$. Observer is located at the distance of $1000\,h^{-1}$ Mpc.

Figure 6 shows that when k is larger than $0.2\,h\,\mathrm{Mpc}^{-1}$, under the plane-parallel approximation, P_p can grow from $\sim 10\%$ to more than 50% larger than P_r; when k is smaller than $0.2\,h\,\mathrm{Mpc}^{-1}$, P_p could still be $> 10\%$ smaller than P_r. Meanwhile, as we expected, with increasing distance of the sample to observer, i.e., with decreasing opening angle, such difference systematically decreases.

However, even when the distance is $1h^{-1}$Gpc which corresponds to an opening angle as small as $\sim 20^\circ$, the systematic bias at $k = 3\,h\,\mathrm{Mpc}^{-1}$ persists around 50%; if one is interested in the highly nonlinear regime, then the bias is also $> 10\%$ for $k < 0.03\,h\,\mathrm{Mpc}^{-1}$ which prevents us from having measurements in *precision*. It is a bad news for most redshift surveys, such as the 2dFGRS redshift survey and the SDSS of which subtended angles are much larger than 20°. Furthermore, as seen in Figures 7 and 8, there are similar systematic biases in reduced bispectrum measured at $k_z = 0$ to the real space bispectrum if we adopt the plane-parallel approximation, the biases not only attenuate the amplitudes but also the configuration dependence.

Therefore, it is hopeless to accurately estimate the real space polyspectra on large scales with the convenient method of using what we measure on the plane $k_z = 0$ in redshift space if no other special skills are applied to correct the systematic bias. One of the possible application of the method is to estimate small scale polyspectra in real space by splitting the wide angle sample into many patches of very small angles in comparison with the scales of interests, and later collecting measurements in these small patches for analysis in precision, which, of course, needs careful numerical experiments to decide the angular widths of those patches (e.g. Park et al. 1994).

4 SUMMARY AND DISCUSSION

In the exploration of the characteristics of redshift distortion in Fourier space, we begin with research on phases of Fourier modes which are rarely noticed in previous works. On very large scales where linear theory applies, phases are not changed by redshift distortion, so we conclude that phase shift $\Delta\theta$ is a nonlinear effect. Then we find that the phase shift by redshift distortion is not deterministic, but it has a distribution function $p(\Delta\theta)$ that is symmetric about its peak at $\Delta\theta = 0$, and qualitatively proportional to (1+const$\cdot\cos\Delta\theta$). The distribution function has strong dependence on the wave length k and the orientation μ of the wave vector to the LOS. More modes are populated around $\Delta\theta = 0$ for small k and small μ.

Limited by the sizes of the available Virgo and VLS simulations and computing resources, we can not obtain reliable $p(\Delta\theta)$ on scales of $k < 0.1\,h\,\mathrm{Mpc}^{-1}$ to build empirical model for the distribution

function. Although in principle it is possible to calculate the phase shift in the perturbation theory, it is unclear as to how to generate the PDF of the phase shift in the perturbation approach, which we leave to future work. Instead we make assumptions on the phase shift at different levels in an effort to depict the redshift distortion on the bispectrum. We discovered that our very crude consideration does provide us with a toy model (Eq. (19)) for the monopole of bispectrum in redshift space, which is in good agreement with numerical simulations on scales $k < 0.2\,h\,\mathrm{Mpc}^{-1}$, and probably can serve as a basis for extended phenomenological models such as Equation (20) and the model in Scoccimarro et al. (1999). If in future an approximation for $p(\Delta\theta)$ analogous to the modeling of amplitude change like Equation (2) can be set with help of large simulations, it is promising that integration of Equation (16) will offer us with greatly improved model for the monopole of bispectrum in redshift space.

On non-linear scales, the plane-wave components of density fluctuation do not evolve independently, and the interaction among different modes leads to the generation of coupled phases. Then, significant phase correlation between different modes is expected. As the Fourier phases of a random Gaussian field are randomly distributed, phase correlation, if any, should characterizes the non-Gaussianity of density fields (Matsubara 2003). Such correlation would have important effects on the bispectrum, which is the lowest order statistics of non-Gaussianity. The connection between phase correlation and non-Gaussianity is undoubtedly important. By using a perturbative quadratic model, Watts & Coles (2003) have shown for the first time how phase association gives rise to non-vanishing bispectrum and three point function in nonlinear processes. The arrangement of phases of modes determines whether such non-Gaussian descriptors are zero or not, but the magnitude of non-Gaussianity is determined by the magnitude of the Fourier modes (Watts & Coles 2003). A relationship between phase correlations and the hierarchy of polyspectra in the Fourier space has been addressed by Matsubara (2003). Also, a numerical test on the bispectrum has been given. However, many details of this issue such as how phase correlation functions with redshift distortion and bias, remain unknown.

The connection between polyspectra and phase information may render us much more useful information, while our knowledge of it is still limited. It is worthwhile for us to tackle the problem in more details by taking into account of both the phase shift of individual Fourier mode discussed in this paper and the correlation between phase shifts of different modes which is overwhelmingly important in understanding the redshift distortion on bispectrum in strong nonlinear regime. As a first step, the simplest consideration on phase shift has already guided us in producing a good model, future inclusion of the PDF and the correlation between phase shift will shed light on the redshift distortion in Fourier space.

In the second part of our report, we explored the goodness of the plane-parallel approximation to the actual radial redshift distortion in Fourier analysis. The first examination is focused on the monopoles of power spectrum and bispectrum. Our measurements with the Virgo and the VLS simulation are consistent with the results of Scoccimarro et al. (2000) that the deviation due to adoption of parallel approximation is $\sim 10\%$ for the monopole of power spectrum and a few percents for bispectrum. Note that the curve in Figure 4 shows a systematic trend toward a higher k. Then, we moved on to check the reliability of the approach of using polyspectra measured on $k_z = 0$ plane as estimation in real space, valid in the plane-parallel approximation. We find that the plane-parallel approximation to radial distortion brings in serious systematic biases: on large scales the "real space" power spectrum from measurements on $k_z = 0$ plane can be overestimated by more than 10%, and it is hugely underestimated by more than 50% on small scales $k >\sim 3\,h\,\mathrm{Mpc}^{-1}$ (Fig. 6). We also find that besides changes in the amplitude of reduced bispectrum, the configuration dependence suffers from the badness of parallel approximation too (Figs. 7 and 8). According to our simulation, such deviation persists even when the opening angle of the sample to the observer is as small as 20°. These discoveries pose serious questions on those claims based on the "real space" polyspectra obtained in this way.

So as long as we are working with monopoles of power spectrum and bispectrum, it is secure to model redshift distortion with plane-parallel approximation. However, if one is going to estimate real space power spectrum and bispectrum with measurements on plane $k_z = 0$, one has to carefully note the caveats of the parallel approximation. Actually a more natural treatment is to decompose the density contrast in redshift space with spherical harmonics and spherical Bessel functions (Heavens & Taylor 1995; Ballinger, Heavens & Taylor 1995; Fisher et al.1995; Szalay, Matsubara & Landy 1998; Percival et al. 2004; Percival 2004; Szapudi 2004).

Acknowledgements Yan-Chuan Cai thanks Prof. Long-Long Feng for support of the work and helpful comments. This work was supported by the National Natural Science Foundation of China through Grant 10373012. Jun Pan appreciates the support by the One-Hundred-Talents program. The simulations in this paper were carried out by the Virgo Supercomputing Consortium using computers based at Computing Center of the Max-Planck Society in Garching and at the Edinburgh Parallel Computing Center. The data are publicly available at www.mpa-garching.mpg.de/NumCos.

References

Chiang L., 2001, MNRAS, 325, 405
Chiang L., 2004, MNRAS, 350, 1310
Chiang L., Coles P., 2000, MNRAS, 311, 809
Chiang L., Coles P., Naselsky P., 2002, MNRAS, 337, 488
Cole S., Fisher K. B., Weinberg D. H., 1995, MNRAS, 275, 515
Cole S., Fisher K. B., Weinberg D. H., 1994, MNRAS, 267, 785
Davis M., Peebles P. J. E., 1983, ApJ, 267, 465
Ballinger W. E., Heavens A. F., Taylor A. N., 1995, MNRAS, 276, 59
Fisher K. B., Davis M., Strauss M. A. et al., 1994, MNRAS, 266, 50
Fisher K. B., Lahav O., Hoffman Y. et al., 1995, MNRAS, 272, 885
Hamilton A. J. S., 1998, In: Astrophysics and space science library (ASSL) Series vol 231, Dordrecht: Kluwer Academic Publishers, p.185
Hamilton A. J. S., Tegmark M., 2002, MNRAS, 330, 506
Hatton S., Cole S., 1998, MNRAS, 296, 10
Hawkins E., et al., 2003, MNRAS, 346, 78
Heavens A. F., Taylor A. N., 1995, MNRAS, 275, 483
Hikage C., Matsubara T., Suto Y., 2004, ApJ, 600, 553
Hikage C., Matsubara T., Suto Y. et al., 2005, PASJ, 57, 709
Hivon E., Bouchet F. R., Colombi S. et al. 1995, A&A, 298, 643
Jenkins A., Frenk C. S., Pearce F. R. et al., 1998, ApJ, 499, 20
Kaiser N., 1987, MNRAS, 227, 1
Matsubara T., 2003, ApJ, 591, L79
Park C., Vogeley M. S., Geller M. J. et al., 1994, ApJ, 413, 569
Peacock J. A., Dodds S. J., 1994, MNRAS, 267, 1020
Percival W. J., Burkey D., Heavens A. et al., 2004, MNRAS, 353, 1201
Percival W. J., 2004, MNRAS, 356, 1168
Saunders W., Rowan-Robinson M., Lawrence A., 1992, MNRAS, 258, 134
Scoccimarro R., 2000, ApJ, 544, 597
Scoccimarro R., Couchman H. M. P., Frieman J. A., 1999, ApJ, 517, 531
Scoccimarro R., 2004, PhRvD, 70, 083007
Szalay A. S., Matsubara T. M., Landy S. D., 1998, ApJ, 498, L1
Szapudi I., 2004, ApJ, 614, 51
Verde L., Heavens A. F., Matarrese S. et al., 1998, MNRAS, 300, 747
Watts P., Coles P., Melott A., 2003, ApJ, 589, L61
Watts P., Coles P., 2003, MNRAS, 338, 806
White M., 2001, MNRAS, 321, 1
Zaroubi S., Hoffman Y., 1996, ApJ, 462, 25